Original Article

Crucial computed tomography and magnetic resonance imaging findings of fallopian tubal tuberculosis for diagnosis: a retrospective study of 26 cases

Zhi-Ying Liang[1,2#^], Ke Zou[1#], Tao-Lin Lin[2#], Jia-Ke Dong[1], Man-Qian Huang[2], Shu-Min Zhou[2], Pei-Qiang Cai[2], Ling Zhang[2], Liang-Jie Li[1]

[1]Department of Radiology, The First People's Hospital of Kashi Area, Kashi, China; [2]Department of Radiology, State Key Laboratory of Oncology in South China, Guangdong Provincial Clinical Research Center for Cancer, Sun Yat-sen University Cancer Center, Guangzhou, China

Contributions: (I) Conception and design: PQ Cai, ZY Liang; (II) Administrative support: K Zou, LJ Li; (III) Provision of study materials or patients: TL Lin, JK Dong, MQ Huang, SM Zhou, K Zou; (IV) Collection and assembly of data: TL Lin, JK Dong, MQ Huang, SM Zhou, K Zou; (V) Data analysis and interpretation: PQ Cai, LJ Li, L Zhang, ZY Liang; (VI) Manuscript writing: All authors; (VII) Final approval of manuscript: All authors.

[#]These authors contributed equally to this work as co-first authors.

Correspondence to: Ling Zhang, PhD. Department of Radiology, State Key Laboratory of Oncology in South China, Guangdong Provincial Clinical Research Center for Cancer, Sun Yat-sen University Cancer Center, Guangzhou 510060, China. Email: zhangl@sysucc.org.cn; Liang-Jie Li, MD. Department of Radiology, The First People's Hospital of Kashi Area, No. 120 Yingbin Avenue, Kashi, China. Email: li507987935@163.com.

Background: Fallopian tubal tuberculosis (FTTB), which typically presents with non-specific clinical symptoms and mimics ovarian malignancies clinically and radiologically, often affects young reproductive females and can lead to infertility if not promptly managed. Early diagnosis by imaging modalities is crucial for initiating timely anti-tuberculosis (anti-TB) treatment. Currently, comprehensive radiological descriptions of this relatively rare disease are limited. We aimed to comprehensively investigate the computed tomography (CT) and magnetic resonance imaging (MRI) characteristics of FTTB in patients from the Kashi area, which has the highest incidence of TB in China, to extend radiologists' understanding of this disease.

Methods: We conducted a retrospective cross-sectional study of 26 patients diagnosed with FTTB at the First People's Hospital of Kashi Area. All the patients underwent abdominal and pelvic contrast-enhanced CT examinations and/or pelvic contrast-enhanced MRI from January 2017 to June 2022. The imaging findings were evaluated in consensus by two experienced radiologists specialized in abdominal and pelvic imaging. The evaluated sites included the fallopian tubes, ovaries, peritoneum, mesentery, retroperitoneal nodes, and parailiac nodes. The patient characteristics are reported using descriptive statistics. The patient imaging results are presented as percentages. The normally distributed continuous variables are reported as the mean ± standard deviation (SD), and otherwise as the median with the interquartile range (IQR).

Results: The median age of the patients was 27 years (IQR: 25–34 years). Bilateral involvement of the fallopian tubes was observed in all patients. The tubal wall appeared coarse with tiny intraductal nodules in 96% (25 of 26) of the patients. The mean CT value of the tubal contents was 34 Hounsfield units (HUs; SD: 3.3 HUs). Ascites was present in 92% (24 of 26) of the patients, with 20 patients showing encapsulated effusion. Among these patients, 20 exhibited the highest CT values of ascites (>20 HUs). Linear enhancement of the parietal peritoneum was observed in 88% (23 of 26) of the patients, of whom

^ ORCID: 0000-0002-8311-5393.

22 had peritoneal nodules measuring a median diameter of 0.4 cm (IQR: 0.3–0.6 cm). Eight patients had retroperitoneal and parailiac nodal enlargement, of whom two showed nodal necrosis, and none displayed nodal calcification.

Conclusions: FTTB is consistently accompanied by tuberculous peritonitis. FTTB typically presents with tubal dilation, and coarseness and nodules in the lumen, as well as intraductal caseous material and calcification. Tuberculous peritonitis exhibits high-density ascites, peritoneal adhesion, linear enhancement of the parietal peritoneum, and tiny peritoneal nodules. The co-occurrence of these features strongly suggests a diagnosis of FTTB.

Keywords: Fallopian tube; female genital organs; tuberculous peritonitis

Submitted May 31, 2023. Accepted for publication Dec 01, 2023. Published online Jan 23, 2024.
doi: 10.21037/qims-23-775
View this article at: https://dx.doi.org/10.21037/qims-23-775

Introduction

Tuberculosis (TB) is an infectious disease caused by the bacillus *Mycobacterium TB* and poses a significant threat to human health (1). In China, where TB is endemic, the Kashi prefecture area in southern Xinjiang has the highest incidence of the disease (2,3). TB typically presents as a pulmonary infection; however, it can also manifest in extrapulmonary forms affecting other parts of the body (1,4). Fallopian tubal tuberculosis (FTTB) is the major manifestation of female genital TB, which is one of the most common forms of extrapulmonary TB (5). FTTB mainly affects young women of reproductive age, and is particularly concerning, as it can result in infertility (6). In regions with a high TB burden, TB-related infertility accounts for up to 24% of cases (7). However, the timely administration of anti-TB treatment and assisted reproduction techniques could restore fertility in approximately 50% of affected individuals (8). Therefore, a timely diagnosis of FTTB is crucial to help preserve fertility.

In clinical practice, patients with FTTB often present with symptoms of abdominal pain and distension. Computed tomography (CT) and magnetic resonance imaging (MRI) are the initial imaging approaches commonly employed to diagnose FTTB. Consequently, a comprehensive understanding of the imaging features of FTTB has great clinical significance. To our knowledge, very few studies have provided descriptions of radiographic findings of FTTB (5,9-12). Currently, there is still a lack of comprehensive radiological descriptions of FTTB derived from a series of cases. FTTB diagnosis is often delayed for several reasons. FTTB usually presents with non-specific clinical symptoms and frequently mimics other diseases clinically and radiologically, particularly ovarian malignancies, which poses significant diagnostic challenges (12,13). As a result, in many cases, positive culture results showing the presence of the TB-causing bacillus *Mycobacterium TB* or positive histopathological findings are required to confirm the diagnosis. However, it may take weeks to obtain a diagnosis based on confirmative laboratory tests. Obtaining samples from the fallopian tubes for diagnostic purposes is both invasive and challenging. Moreover, histopathological evidence of tuberculous granulomas is only found in a minority of cases (14-16). In such clinical contexts, non-invasive radiological imaging modalities, such as CT and MRI, play a crucial role in facilitating the early detection and diagnosis of FTTB.

In the present study, we conducted a thorough review of CT and MRI images of 26 patients with confirmed FTTB. Our aim was to comprehensively evaluate the imaging features of FTTB in patients from Kashi area, using the largest sample size known to date, to extend radiologists' understanding of this disease. We present this article in accordance with the STROBE reporting checklist (available at https://qims.amegroups.com/article/view/10.21037/qims-23-775/rc).

Methods

Patients

The study was conducted in accordance with the Declaration of Helsinki (as revised in 2013). The study was approved by the Institutional Ethics Committee of the First People's Hospital of Kashi Area {Approval No: Expedited ethical approval No. 81 [2023]}, and the requirement of

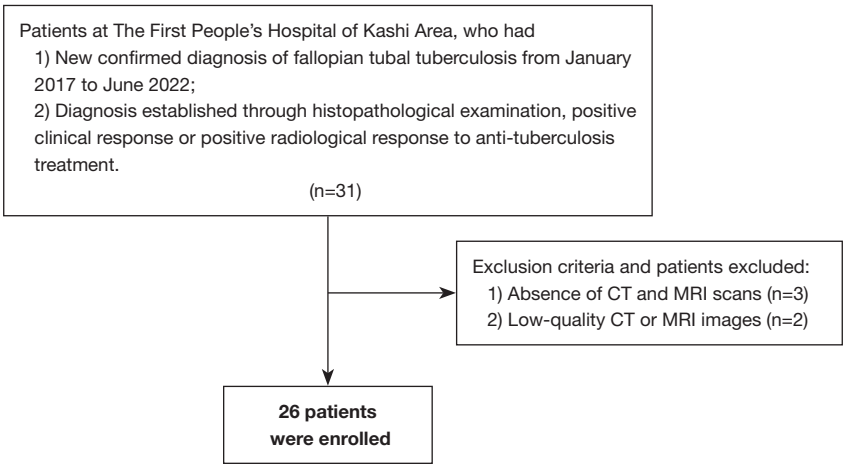

Figure 1 Flow diagram showing patient selection. CT, computed tomography; MRI, magnetic resonance imaging.

individual consent for this retrospective analysis was waived. We retrospectively reviewed and evaluated the imaging data of 26 patients with confirmed FTTB who underwent at least one CT or MRI examination between January 2017 and June 2022; imaging data were unavailable prior to 2017 due to a system-wide upgrade of our picture archiving and communication system (PACS, Syngo MultiModality Workplace, Siemens, Erlangen, Germany). Patients were excluded from the study for the following reasons: they did not undergo CT and MRI examinations; and/or they had low-quality CT or MRI images that could not be used for proper diagnostic assessment. *Figure 1* shows the flow of patient selection.

A diagnosis of FTTB was confirmed based on a histopathological examination, or a positive clinical or radiological response to anti-TB treatment. For the patients who underwent a histopathological examination, their pathology specimens were meticulously assessed by a dedicated pathologist with over 10 years of specialized expertise in abdominal and pelvic pathology. The other data collected from the electronic medical records included patient age, history of pulmonary TB, clinical symptoms (including abdominal pain, abdominal distension, and tuberculous toxic symptoms), and laboratory examination results [including the leukocyte count, erythrocyte sedimentation rate (ESR), and serum cancer antigen 125 (CA-125) level].

CT and MRI protocols

The radiological examinations were conducted before treatment initiation. Contrast-enhanced abdominal and pelvic CT scans were performed (SOMATOM Definition, Siemens). The reconstructed slice thickness was 1 mm, with an increment of 0.5 mm. Imaging was conducted in the hepatic arterial phase, portal venous phase, and delay phase, following the intravenous administration of a bolus dose of 90 mL of non-ionic iodinated contrast agent at a rate of 5 mL/s. Further, in addition to abdominal and pelvic scans, chest CT scans were conducted on most patients to investigate their history of pulmonary TB.

Pelvic MRI examinations were performed using a 1.5-T scanner (MAGNETOM Aera, Siemens). The imaging sequence parameters were as follows: (I) fast spin-echo T2-weighted imaging in both the axial and coronal planes with a repetition time/echo time range of 3,000–6,000/50–80 ms; (II) spin-echo T1-weighted imaging in the axial plane with a repetition time/echo time range of 500–750/7–10 ms; and (III) post-contrast gadolinium-enhanced spin-echo T1-weighted imaging with a repetition time/echo time range of 500–750/7–10 ms in all three orthogonal planes following the intravenous injection of 0.1 mmol of gadolinium per kilogram of body weight. The remaining important scanning parameters included a field of view measuring 23 cm × 32 cm and a matrix size of 256×320. None of the patients experienced any adverse events related to the use of the contrast agents during the CT and MRI examinations.

Imaging analysis

Of the 26 patients included in the study, 23 underwent contrast-enhanced CT examinations, and 11 underwent

Table 1 Clinical characteristics of all 26 patients with fallopian tubal tuberculosis

Characteristic	Value
Imaging modality	
CT	23 (88%)
MRI	11 (42%)
Diagnosis approach	
Histopathological examination	11 (42%)
Positive response to anti-tuberculosis treatment	15 (58%)
Age (years)	27 [25–34]
Clinical presentation	
Abdominal pain	19 (73%)
Abdominal distension	22 (85%)
Tuberculous toxic symptoms	12 (46%)
Laboratory examination*	
High leucocyte count ($\times 10^9$/L)	4 (18%), 7 [6–9]
High ESR (mm/h)	9 (60%), 36 [14–64]
High serum CA-125 level (U/mL)	17 (89%), 217 [112–407]
History of pulmonary tuberculosis*	9 (50%)

Data are presented as n (%) or median [IQR]. *, Clinical characteristics, including leucocyte count, ESR, serum CA-125 level, and history of pulmonary tuberculosis, were available for 22, 15, 19, and 18 patients, respectively. CT, computed tomography; MRI, magnetic resonance imaging; ESR, erythrocyte sedimentation rate; CA-125, cancer antigen 125; IQR, interquartile range.

contrast-enhanced MRI examinations. Three patients only underwent MRI examinations, and eight patients underwent both CT and MRI examinations. Two radiologists (L.J.L. and P.Q.C., with 5 and 10 years of experience in abdominal and pelvic imaging diagnosis, respectively) evaluated the CT and MRI images in consensus using a PACS.

The fallopian tubes and ovaries were evaluated for various manifestations, including the laterality of tubal involvement, size of the largest lesion, presence of simple tubular dilatation or tubo-ovarian mass (comprising the adhesion of the fallopian tube and ovary), maximum diameter of the dilated tube, uniformity or coarseness of the tubal wall, diameter of the largest intraluminal nodule, CT value of the tubal contents, presence of tubal calcification, presence of ovarian calcification, and presence of peritubal adhesions. The CT value of the tubal contents (excluding calcification) was measured in Hounsfield units (HUs) by averaging the values obtained from three circular regions of interest (ROIs), each measuring 20–25 mm^2. Instances of tubal wall rupture were also recorded when observed.

The abdominal evaluation comprised an assessment of ascites (presence or absence, free or encapsulated type, and the highest CT value), linear enhancement of the parietal peritoneum, and the largest diameter of peritoneal nodules (except for calcified nodules). The presence of intestinal obstruction, peritoneal calcification, and mesenteric nodal calcification were also documented. When assessing the highest CT value of ascites, we averaged the values obtained from three ROIs placed on the lowest sites of ascites where caseous necrosis and/or cell disintegration might deposit.

Further, findings related to the retroperitoneal and parailiac lymph nodes, including enlargement, calcification, necrosis, and the maximum short diameter of the largest node, were also recorded.

Statistical analysis

The patient characteristics are reported using descriptive statistics. The patient imaging results are presented as percentages. The normally distributed continuous variables are reported as the mean ± standard deviation (SD), and otherwise as the median with the interquartile range (IQR). The statistical analyses were conducted using SPSS version 25 (IBM, Armonk, New York, USA).

Results

Characteristics and clinical symptoms of the patients

A total of 26 patients were included in this study, and their characteristics and clinical symptoms are summarized in *Table 1*. A diagnosis of FTTB was confirmed by histopathological examinations in 11 cases (42%), and positive clinical or radiological responses to anti-TB treatment in 15 cases (58%). The patients had a median age of 27 years (IQR: 25–34 years). The most common clinical symptoms were abdominal distension (85%) and abdominal pain (73%). Elevated ESR levels were observed in 60% of the 15 patients tested, with a median value of 36 mm/h (IQR: 14–64 mm/h). Elevated CA-125 levels were observed in 89% of the 19 patients tested, with a median value of 217 U/mL (IQR: 112–407 U/mL).

Table 2 CT and MRI findings of fallopian tubal tuberculosis: manifestations of fallopian tubes and ovaries

Patient No.	Age (years)	Laterality of tubal involvement*	Size of the largest lesion (cm × cm)	Simple tubal dilatation [0], tubo-ovarian mass [1]	Max. diameter of tubal dilatation (cm)	Tubal wall[&]	Diameter of the largest intraluminal nodule (cm)	CT value of tubal contents (HU)	Tubal calcification[†]	Ovarian calcification[†]	Peritubal adhesions[†]
1	26	1	3.3×6.7	1	1.9	1	0.5	31	0	0	1
2	45	1	2.9×4.4	1	0.5	1	0.2	40	0	0	1
3	27	1	3.5×3.8	1	1.2	1	0.5	32	0	0	1
4	22	1	4.3×4.6	1	0.9	1	0.4	33	0	1	1
5	27	1	8.4×7.8	1	7.8	1	0.4	30	1	1	1
6	34	1	3.4×4.0	1	0.7	1	0.3	30	1	1	1
7	25	1	2.3×4.1	1	1.5	1	0.4	36	0	0	1
8	38	1	4.3×4.5	1	2.1	1	0.5	33	0	0	1
9	27	1	6.2×3.7	1	1.2	1	0.4	40	1	1	1
10	21	1	3.1×5.9	1	1.2	1	0.5	33	0	0	1
11	26	1	4.3×6.6	1	2.6	1	0.3	37	0	0	1
12	34	1	4.7×4.6	1	1.1	1	0.3	31	1	1	1
13[‡]	21	1	6.3×3.3	1	2.8	1	0.3	NA	NA	NA	1
14	28	1	4.9×3.4	1	2.3	1	0.3	35	0	0	1
15[‡]	31	1	4.6×4.7	1	0.7	1	0.3	NA	NA	NA	1
16	27	1	1.7×3.5	1	0.6	1	0.3	41	1	0	1
17	37	1	3.3×4.9	1	1.1	1	0.3	34	0	0	1
18	31	1	3.1×3.8	1	1.3	1	0.3	35	0	0	1
19	30	1	4.6×7.3	1	1.7	1	0.3	31	0	0	1
20[‡]	19	1	8.3×5.1	1	3.1	1	0.3	NA	NA	NA	1
21	25	1	5.3×4.8	1	1.4	1	0.3	35	0	0	1
22	19	1	3.3×3.5	1	1.1	1	0.3	30	1	0	1
23	26	1	3.7×4.6	1	0.9	1	0.3	34	0	0	1
24	47	1	5.4×3.7	0	0.4	0	0	38	1	1	1
25	34	1	4.9×3.2	1	0.7	1	0.3	33	0	0	1
26	62	1	9.2×6.9	1	4.1	1	0.2	33	0	0	1

*, unilateral [0], bilateral [1]; [†], means the value in the column is recorded as negative [0] and positive [1]; [&], uniform [0], coarse [1]; [‡], means only MRI examination data were available. CT, computed tomography; MRI, magnetic resonance imaging; HU, Hounsfield unit; NA, not applicable.

Imaging manifestations of fallopian tubes and ovaries in FTTB

The manifestations of FTTB in all patients are presented in *Table 2*. All the patients presented with bilateral involvement and dilation of the fallopian tubes (as indicated by the blue arrows in *Figures 2-4*), with a median maximum dilatation diameter of 1.2 cm (IQR: 0.9–2.2 cm). A tubo-ovarian mass was observed in 96% (25 of 26) of the patients (*Figure 3*). In 96% (25 of 26) patients, the tubal wall displayed coarseness with intraductal nodules, with a median nodular size of 0.3 cm (IQR: 0.3–0.4 cm) (*Figure 4*). The mean CT value of the tubal contents, available for 23 patients, was 34 HUs with a SD of 3.3 HUs (*Figure 4D*). Tubal calcification was observed in 30% (7 of 23) of the patients, and ovarian calcification was observed in 26% (6 of 23) of the patients (*Figure 5A,5B*). Tubal rupture was observed in only one patient (*Figure 5C,5D*).

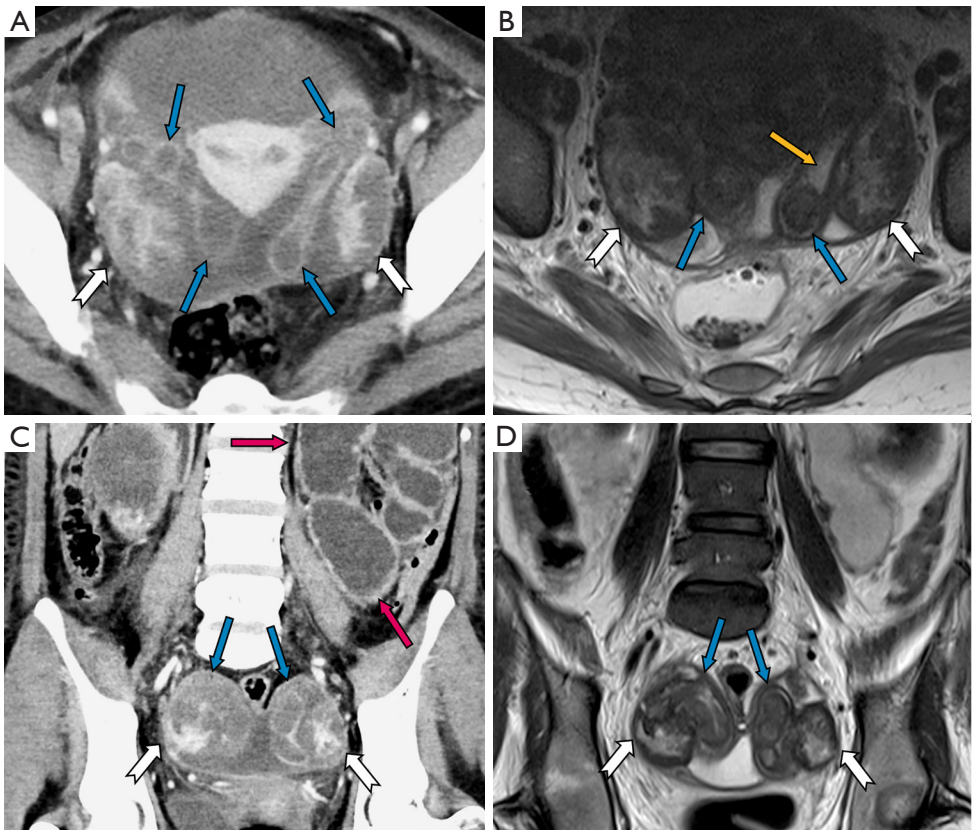

Figure 2 Images of a 25-year-old female (patient No. 7) diagnosed with fallopian tubal tuberculosis with tuberculous peritonitis. The panel includes axial post-contrast CT (A) and T2-weighted MRI (B) images, as well as coronal post-contrast CT (C), and T2-weighted MRI (D) images. The bilateral fallopian tubes are dilated (as indicated by the blue arrows in all the images) and filled with intraductal caseous material and pyosalpinx (as indicated by the gold arrow in image B). The left fallopian tube shows a characteristic beaded appearance (C, D). The fallopian tubes, ovaries (as indicated by the swallow-tail arrows in all the images), and parietal peritoneum adhere to each other. The small intestines are dilated and filled with fluid, which indicates obstruction (as indicated by the magenta arrow in image C). CT, computed tomography; MRI, magnetic resonance imaging.

Imaging manifestations of accompanying signs in FTTB: tuberculous peritonitis

The manifestations of tuberculous peritonitis are presented in *Table 3*. Ascites was observed in 92% (24 of 26) of the patients, with 83% of these patients (20 of 24) presenting with encapsulated effusion. Among the 22 patients for whom the highest CT values of ascites were available, the median value was 24 HUs (IQR: 22–25 HUs), and 91% (20 of 22) had values above 20 HUs (*Figure 4D*). Linear enhancement of the parietal peritoneum was observed in 88% (23 of 26) of the patients (*Figure 3A,3D-3F*). Peritoneal nodules were found in 85% (22 of 26) of the patients (*Figure 4F*), with the median diameter of the largest peritoneal nodules measuring 0.4 cm (IQR: 0.3–0.6 cm). Intestinal obstruction occurred in 23% (6 of 26) of the patients (*Figure 2C*).

Imaging manifestations of accompanying signs in FTTB: retroperitoneal and parailiac lymphadenopathy

The manifestations of retroperitoneal and parailiac lymphadenopathy are detailed in *Table 3*. Enlarged nodes were observed in eight patients (*Table 3*, *Figure 6*). The mean maximum short diameter of the largest nodes was 1.3 cm (SD: 0.24 cm). Among these patients, two had necrotic

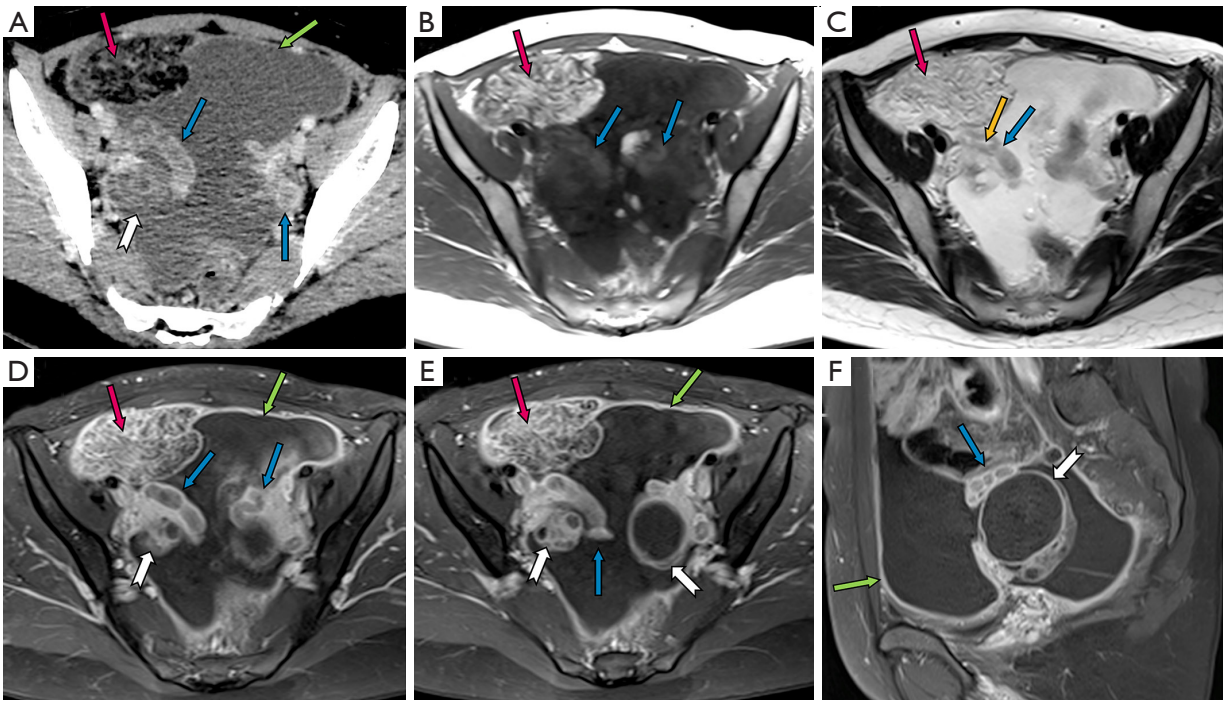

Figure 3 Images of a 22-year-old female (patient No. 4) diagnosed with fallopian tubal tuberculosis with tuberculous peritonitis. The panel includes axial post-contrast CT (A), T1-weighted MRI (B), T2-weighted MRI (C), post-contrast T1-weighted MRI (D,E), and sagittal post-contrast T1-weighted MRI (F) images. The bilateral fallopian tubes are dilated (as indicated by the blue arrows in all the images), filled with intraductal caseous material, and pyosalpinx (as indicated by the gold arrow in image C). The caseous material shows mild, high signal intensity on T1-weighted images, probably due to the presence of lipids inside. It shows iso-signal or mild, low signal intensity on T2-weighted images, without corresponding contrast enhancement. The thickness of the right fimbriae of fallopian tube can be observed (as indicated by the blue arrow in image E). Adhesion of the ovaries can be observed (as indicated by the swallow-tail arrows in images A, D, E, and F). The left fallopian tube has a beaded appearance (as indicated by the blue arrow in image F). Tuberculous peritonitis manifests as ascites, thickness and adhesion of the greater omentum (as indicated by the magenta arrows in images A, B, C, D, and E), and linear enhancement of the parietal peritoneum without evident nodules on it (as indicated by the green arrows in images A, D, E, and F). CT, computed tomography; MRI, magnetic resonance imaging.

nodes (*Figure 6D*). No nodal calcification was observed.

Discussion

The early diagnosis of FTTB can facilitate the prompt initiation of anti-TB treatment, potentially preserving fertility in affected patients. This article provides comprehensive CT and MRI descriptions of FTTB from 26 patients. We observed that FTTB is always accompanied by tuberculous peritonitis. FTTB is characterized by specific features, such as tubal dilation, coarseness and nodules in the lumen, intraductal caseous material, and calcification. Tuberculous peritonitis manifests with high-density ascites, peritoneal adhesion, linear enhancement of the parietal peritoneum, peritoneal calcification, tiny peritoneal nodules, and mesenteric lymphadenopathy. The combined presence of these features is highly suggestive of a diagnosis of FTTB.

In FTTB, the most noticeable radiological feature is the tubal dilatation, which was observed in all the patients in our study. The dilation can be quite significant and is attributed to various factors such as hydrosalpinx, pyosalpinx, the presence of caseous material, and tubal adhesions. Tubal rupture is a rare complication in severe cases, as evidenced by there being only one occurrence in our study (*Figure 5C,5D*). Dilated tubes vary morphologically, presenting with C-shaped, S-shaped, rigid pipe-shaped or multilocular cystic appearances. In addition, we noted

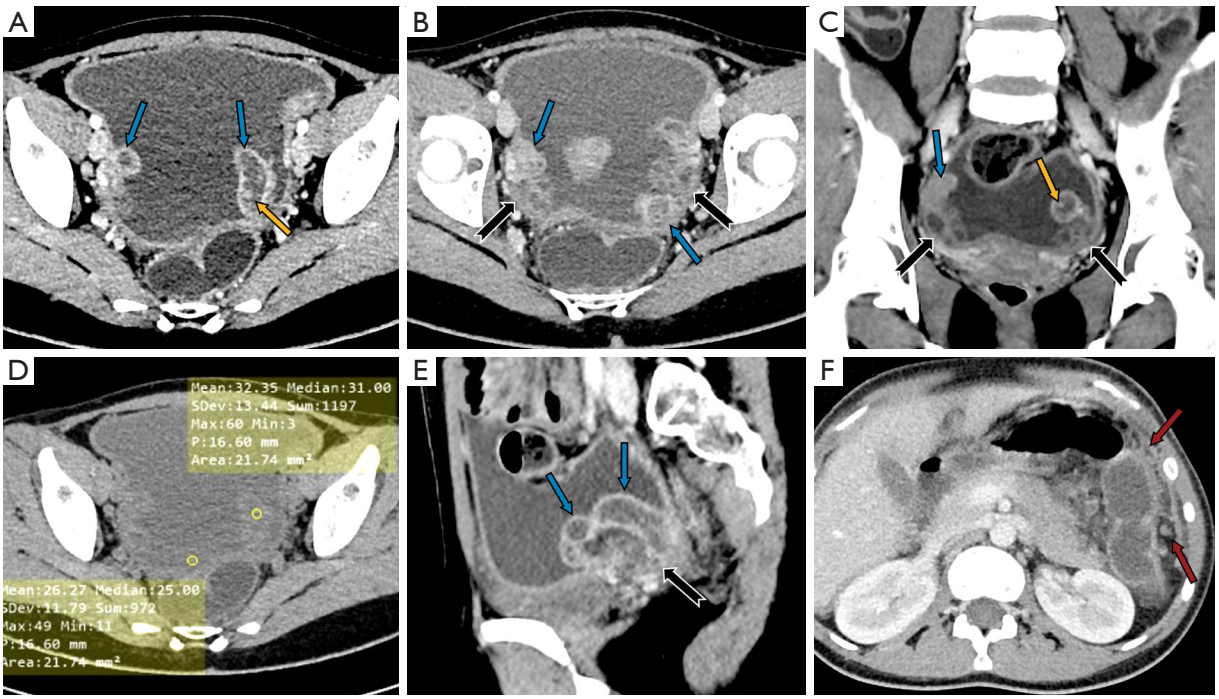

Figure 4 Images of a 21-year-old female (patient No. 10) diagnosed with fallopian tubal tuberculosis with tuberculous peritonitis. The panel includes axial post-contrast CT (A,B,F), coronal post-contrast CT (C), sagittal post-contrast CT (E), and axial plain CT (D) images. The bilateral fallopian tubes are dilated (as indicated by the blue arrows in A, B, C, and E), with intraductal caseous material (the upper ROI in image D, the CT value is 32 HUs). The tubal wall is coarse with intraluminal nodules (as indicated by the gold arrows in images A and C). The fallopian tubes, ovaries (as indicated by the swallow-tail arrows in images B, C, and E), and parietal peritoneum adhere to each other. The CT value of ascites is 26 HUs (the lower ROI in image D). Nodular and stripe-like thickening of the peritoneum can be observed (as indicated by the red arrows in image F). CT, computed tomography; HUs, Hounsfield units; ROI, region of interest.

coarse tubal walls with tiny and enhanced intraductal nodules in most patients (25 of 26), which were attributed to the formation of tuberculous granulomas and subsequent caseous ulceration during the acute tuberculous endosalpingitis. These findings align with those of a previous study that suggested that FTTB primarily presents in the acute exudative and productive adhesive stages (17,18). We noted peritubal adhesions in all patients, which presented either as inter-tubal adhesions or adhesions between tubes and abdominopelvic organs or the parietal peritoneum. With the help of MRI for localization, we determined that the mean CT value of caseous material was 34 HUs (SD: 3.3). The caseous material can calcify, resulting in the formation of tiny high CT density nodules or linear streak-like calcifications along the tubes (17). Therefore, tubal calcification serves as a characteristic feature for the diagnosis of FTTB; however, it was only observed in 30% (7 of 23) of the patients who had CT examinations in our study.

In our study, we observed a significant co-occurrence of tuberculous peritonitis with FTTB in a significant proportion of patients (25 of 26). This simultaneous presence of FTTB and tuberculous peritonitis can be attributed to the anatomical connection between the lumens of the fallopian tubes and the peritoneal cavity. In cases of FTTB, the disease can extend into the peritoneum, and conversely, tuberculous peritonitis can involve the lumens of the fallopian tubes. In our study, 91% of the patients had ascites with CT values exceeding 20 HUs. Consistent with previous findings (19,20), this elevated CT value indicates the high protein and cellular content of the fluid. Ascites presenting as encapsulated effusion was a common observation in 83% of the 24 patients with ascites, which suggests that adhesions are frequently present in cases of tuberculous peritonitis. These adhesions result from significant fibrous tissue proliferation, and they can lead to intestinal obstruction in severe situations. We identified six cases of intestinal obstruction in our study. Three of these

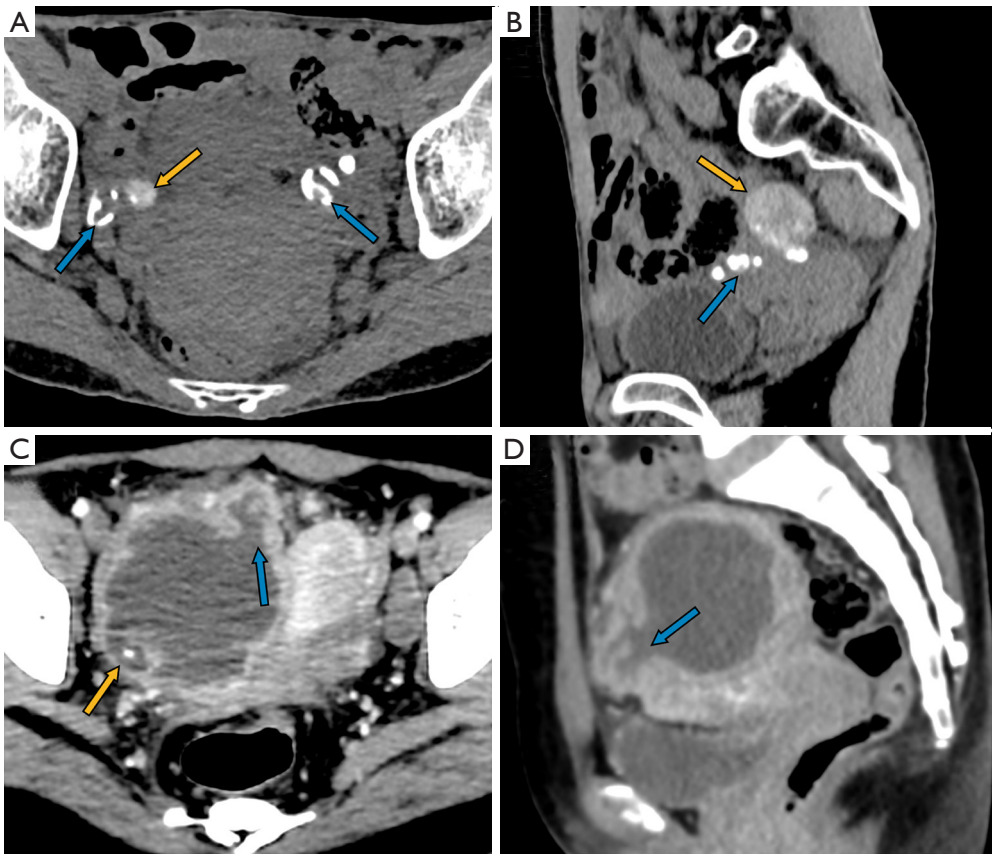

Figure 5 Imaging findings of two patients diagnosed with fallopian tubal tuberculosis. (I) Patient No. 24, a 47-year-old female (A,B). Axial (A) and sagittal (B) plain CT images are presented. Nodular calcification along the course of bilateral fallopian tubes (as indicated by the blue arrows) and calcification of the bilateral ovaries (as indicated by the gold arrows) can be observed. (II) Patient No. 5, a 27-year-old female. Axial (C) and sagittal (D) post-contrast CT images are presented. The right fallopian tube is obviously dilated, and a rupture of the tubal wall can be observed (as indicated by the blue arrows in images C and D). Calcification in the tube can be observed (as indicated by the gold arrow in image C). CT, computed tomography.

cases were incidentally detected during abdominal CT examinations conducted due to acute intestinal obstruction symptoms, which revealed the presence of FTTB. The remaining three patients presented with chronic and progressive symptoms of abdominal distension and pain. Among these six patients with intestinal obstruction, three exhibited mild intestinal wall edemas, and all the patients displayed ileus adhesions. Therefore, when encountering cases of intestinal obstruction in clinical practice, it is also important to consider the possibility of tuberculous peritonitis and genitourinary TB, especially in endemic areas. Another common characteristic feature of tuberculous peritonitis that we observed is linear enhancement of the parietal peritoneum. This finding is consistent with a previous study (12). Additionally, we noted a relatively high rate of peritoneal nodules (85%), which appeared as small nodular foci with a patchy distribution. Calcified peritoneal nodules, a characteristic feature of tuberculous peritonitis, were present in 30% of our patients.

With better soft tissue contrast resolution than CT, MRI offers superior visualization of the internal caseous materials and the tubal morphology. Caseous material shows mild, high signal intensity on T1-weighted images, and iso-signal or mild, low signal intensity on T2-weighted images, with no corresponding contrast enhancement. On MRI, the fallopian tubes have a distinctive beaded appearance due to the nodular caseous materials with intraluminal adhesions. Conversely, CT excels in the visualization of calcifications. Given the frequent use of CT in assessing acute or chronic abdominal conditions, it is crucial that clinicians are able to

Table 3 CT and MRI findings of accompanying signs in fallopian tubal tuberculosis: tuberculous peritonitis, retroperitoneal, and parailiac lymphadenopathy

Patient No.	Age (years)	Tuberculous peritonitis							Retroperitoneal and parailiac lymphadenopathy				
		Free ascites†	Encapsulated ascites†	Highest CT value of ascites (HU)	Linear enhancement of the parietal peritoneum†	Largest peritoneal nodule (cm)	Peritoneal calcification†	Mesenteric nodal calcification†	Enlarged retroperitoneal lymph node†	Enlarged parailiac lymph node†	Retroperitoneal nodal calcification†	Parailiac nodal necrosis†	Maximum short diameter of the largest lymph node (cm)
1	26	1	1	23	1	0.4	0	0	1	1	0	0	1.1
2	45	1	1	25	1	0.3	1	0	0	0	0	0	0
3	27	1	1	23	1	0.6	0	0	0	0	0	0	0
4	22	1	1	24	1	0.5	0	0	0	0	0	0	0
5	27	0	0	NA	0	0	0	1	1	1	0	1	1.5
6	34	1	1	24	1	0.3	1	1	0	0	0	0	0
7	25	1	1	30	1	0.3	0	0	1	1	0	0	1.3
8	38	1	1	21	1	0.8	0	0	1	1	0	0	1.2
9	27	1	1	22	1	0.8	1	0	1	1	0	0	1.4
10	21	1	1	24	1	0.6	0	0	0	0	0	0	0
11	26	1	1	25	1	0.3	0	0	0	0	0	0	0
12	34	1	1	23	1	0	0	0	0	0	0	0	0
13‡	21	1	1	NA	1	0.3	NA	NA	0	0	0	0	0
14	28	1	1	25	1	0.5	0	0	0	0	0	0	0
15‡	31	0	0	NA	0	0	NA	NA	0	0	0	0	0
16	27	1	1	23	1	0.3	1	1	0	0	0	0	0
17	37	1	1	25	1	0.4	0	0	0	0	0	0	0
18	31	0	1	25	1	0.3	0	0	1	1	0	0	1.0
19	30	1	1	22	1	0.4	1	0	0	0	0	0	0
20‡	19	1	1	NA	1	0.3	NA	NA	0	0	0	0	0
21	25	1	0	16	1	0.5	0	0	0	0	0	0	0
22	19	1	1	24	1	0.7	0	0	0	0	0	0	0
23	26	1	1	22	1	0.9	0	0	1	1	0	1	1.1
24	47	1	0	25	0	0	1	1	0	0	0	0	0
25	34	1	0	27	1	0.2	1	0	0	0	0	0	0
26	62	1	0	14	1	0.4	0	0	1	1	0	0	1.7

†, means the value in the column is recorded as negative [0] and positive [1]; ‡, means only the MRI examination data were available. CT, computed tomography; MRI, magnetic resonance imaging; HU, Hounsfield unit; NA, not applicable.

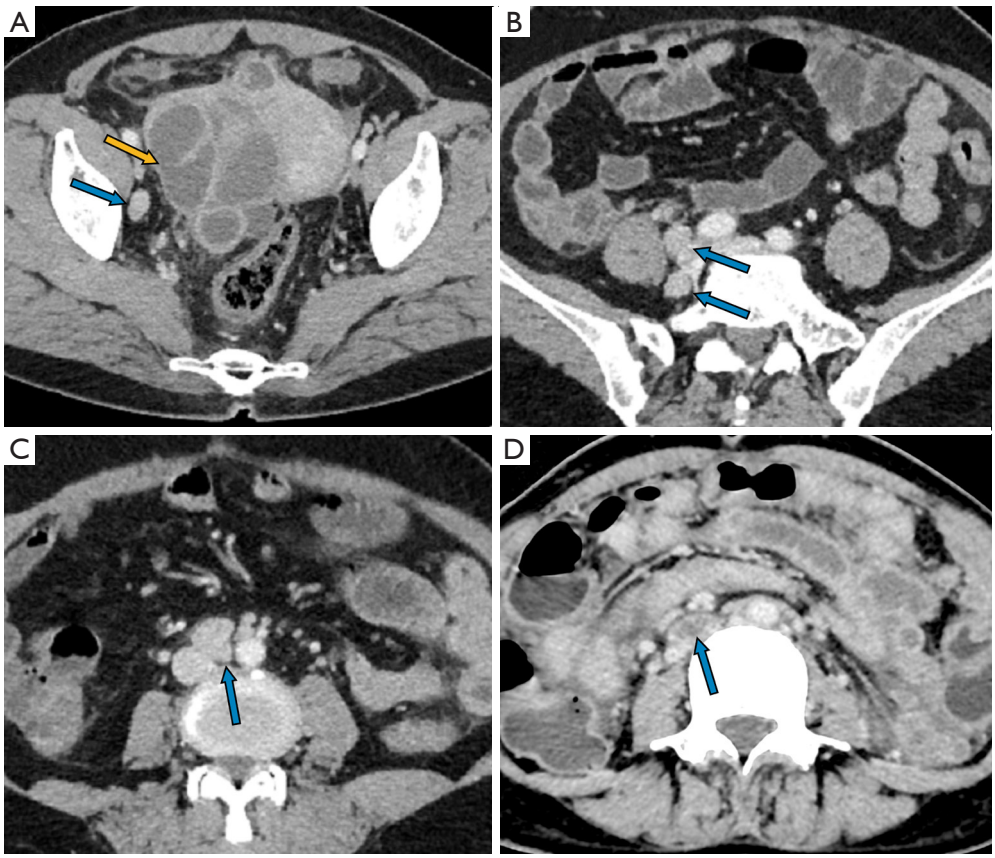

Figure 6 Axial post-contrast CT findings of two patients diagnosed with fallopian tubal tuberculosis. (I) Patient No. 26, a 62-year-old female. Axial post-contrast CT (A-C) images are presented. Image A shows a right cystic adnexal mass with an incomplete septa (as indicated by the gold arrow). There are enlarged right parailiac and aortocaval lymph nodes (as indicated by the blue arrows in images A, B and C) characterized by clearly bordered, homogeneous, and marked enhancement. (II) Patient No. 23, a 26-year-old female. The single axial postcontrast CT image (D) shows necrotic lymph nodes within the aortocaval group (as indicated by the blue arrow in image D). CT, computed tomography.

recognize the signs of FTTB on CT scans.

It Is often challenging to distinguish FTTB from other pelvic malignancies, such as ovarian cancer; thus, careful differential diagnosis is critical. Fallopian tubal cancer or ovarian cancer involving the fallopian tube often presents with larger soft tissue nodules in the tubal lumen. Conversely, tuberculous tubo-ovarian masses exhibit smaller solid soft tissue foci in the adnexal areas. A previous study by Ludovisi *et al.* (21) noted specific ultrasound characteristics that might indicate tubal cancer, including a well-vascularized ovoid or sausage-shaped structure, either completely solid or with large solid components in the pelvis. In our study of the CT/MRI features of FTTB, the fallopian tubes displayed a characteristic beaded appearance without significant solid components, which should aid in the differentiation between tubal cancer and tubal TB. Surprisingly, among our cases, none of the eight patients (31%, 8 of 26) with enlarged retroperitoneal and peritoneal nodes showed calcification, and two patients exhibited nodal necrosis. In our experience, metastatic retroperitoneal nodes in ovarian cancer tend to have a higher likelihood of necrosis and larger size. All patients in our study presented with bilateral tubal lesions, and 96% exhibited adhesions to the ovaries, forming indistinct masses. Therefore, when FTTB is accompanied by tuberculous peritonitis, the primary consideration in the differential diagnosis should be ovarian cancer with peritoneal implantation metastasis.

Adhesions caused by FTTB are typically more prominent than those caused by ovarian cancer (10). Lesions associated with peritoneal implantation metastasis are usually rounder

and larger than those associated with tuberculous peritonitis. Important CT/MRI findings, including high-density ascites, peritoneal calcification, linear enhancement of the parietal peritoneum, and small peritoneal nodules, are essential for distinguishing tuberculous peritonitis from ovarian cancer with peritoneal implantation metastasis. Similarly, Ludovisi *et al.* (22) reported a case in which pelvic TB was initially misdiagnosed as peritoneal carcinoma, which emphasizes the importance of considering the possibility of peritoneal TB, in addition to peritoneal carcinoma, when ultrasonography and CT scans reveal features, such as peritonitis, adnexal masses, omental thickening, and ascites. In the assessment of pelvic masses, ultrasound can achieve more than 90% accuracy in distinguishing between benign and malignant adnexal masses (23). As it exhibits satisfactory concordance with laparoscopy in assessing ovarian and peritoneal cancer (24,25), ultrasound can significantly help the differential diagnosis of pelvic masses and pelvic TB, particularly in cases in which the CT or MRI evidence is insufficient.

Clinical features offer limited diagnostic clues for differentiating between FTTB combined with tuberculous peritonitis, and ovarian cancer combined with peritoneal implantation metastasis. Tjahyadi *et al.* (26) previously observed that chronic lower abdominal and pelvic pain is a common symptom in patients with female genital TB. This can often be accompanied by pelvic masses, cysts, abscesses, vaginal pain, menstrual dysfunction, dysmenorrhea, and postpartum pain. Both conditions (i.e., FTTB and ovarian cancer with peritoneal implantation metastasis) may result in elevated ESR, along with symptoms like abdominal distension and pain. In our study, 46% of the patients showed symptoms of TB intoxication. Additionally, the CA-125 levels were elevated in 89% of the patients, resembling findings in late-stage ovarian cancer (89%). However, in contrast to the significantly higher levels observed in ovarian cancer (27), our patients exhibited a moderately elevated median value of 217 U/mL (IQR: 112–407 U/mL). Thus, emphasizing the numerical value of CA-125, rather than relying solely on its presence above a specific threshold, is crucial in the differential diagnosis process.

Our study had certain limitations. First, only 42% of the cases were pathologically confirmed as FTTB, while the remaining cases were indirectly confirmed based on the effectiveness of the anti-TB treatment. Second, MRI examinations were conducted in only 42% of the patients due to economic constraints; MRI is a more expensive imaging modality than CT. Finally, our study population was relatively small, which was largely due to the referral patterns of our comprehensive hospital. Patients with suspected TB based on initial imaging reports were commonly transferred to specialized infectious disease hospitals for further management. Consequently, we were unable to obtain the final diagnoses of these transferred patients, resulting in their exclusion from our study. However, to our knowledge, our study still comprised the largest sample size for presenting comprehensive imaging features of FTTB. We plan to increase our sample size through prospective data collection in the future.

Conclusions

CT and MRI examinations can reveal the characteristic features of FTTB. It is important to note that FTTB is always accompanied by tuberculous peritonitis. Combining the features of FTTB and tuberculous peritonitis enables an accurate and timely diagnosis, facilitating appropriate clinical management and preserving fertility in affected individuals.

Acknowledgments

The authors would like to thank the staff of the Department of Radiology of The First People's Hospital of Kashi Area for their valuable support.
Funding: None.

Footnote

Reporting Checklist: The authors have completed the STROBE reporting checklist. Available at https://qims.amegroups.com/article/view/10.21037/qims-23-775/rc

Conflicts of Interest: All authors have completed the ICMJE uniform disclosure form (available at https://qims.amegroups.com/article/view/10.21037/qims-23-775/coif). The authors have no conflicts of interest to declare.

Ethical Statement: The authors are accountable for all aspects of the work in ensuring that any questions related to the accuracy or integrity of any part of the work have been appropriately investigated and resolved. The study was conducted in accordance with the Declaration of Helsinki (as revised in 2013). The study was approved by the Institutional Ethics Committee of the First People's Hospital of Kashi Area {Approval No: Expedited ethical

approval No. 81 [2023]}, and the requirement of individual consent for this retrospective analysis was waived.

References

1. Bagcchi S. WHO's Global Tuberculosis Report 2022. Lancet Microbe 2023;4:e20.
2. Tusun D, Abulimiti M, Mamuti X, Liu Z, Xu D, Li G, Peng X, Abudureyimu T, Zhang L, Zhao Y, Ou X. The Epidemiological Characteristics of Pulmonary Tuberculosis - Kashgar Prefecture, Xinjiang Uygur Autonomous Region, China, 2011-2020. China CDC Wkly 2021;3:557-61.
3. Hu M, Feng Y, Li T, Zhao Y, Wang J, Xu C, Chen W. Unbalanced Risk of Pulmonary Tuberculosis in China at the Subnational Scale: Spatiotemporal Analysis. JMIR Public Health Surveill 2022;8:e36242.
4. Rodriguez-Takeuchi SY, Renjifo ME, Medina FJ. Extrapulmonary Tuberculosis: Pathophysiology and Imaging Findings. Radiographics 2019;39:2023-37.
5. Sharma JB. Current Diagnosis and Management of Female Genital Tuberculosis. J Obstet Gynaecol India 2015;65:362-71.
6. Sharma JB, Sharma E, Sharma S, Dharmendra S. Female genital tuberculosis: Revisited. Indian J Med Res 2018;148:S71-83.
7. Singh N, Sumana G, Mittal S. Genital tuberculosis: a leading cause for infertility in women seeking assisted conception in North India. Arch Gynecol Obstet 2008;278:325-7.
8. Jindal UN, Verma S, Bala Y. Favorable infertility outcomes following anti-tubercular treatment prescribed on the sole basis of a positive polymerase chain reaction test for endometrial tuberculosis. Hum Reprod 2012;27:1368-74.
9. Naeem M, Zulfiqar M, Siddiqui MA, Shetty AS, Haq A, Varela C, Siegel C, Menias CO. Imaging Manifestations of Genitourinary Tuberculosis. Radiographics 2021;41:1123-43.
10. Sharma JB, Jain SK, Pushparaj M, Roy KK, Malhotra N, Zutshi V, Rajaram S. Abdomino-peritoneal tuberculosis masquerading as ovarian cancer: a retrospective study of 26 cases. Arch Gynecol Obstet 2010;282:643-8.
11. Barutcu O, Erel HE, Saygili E, Yildirim T, Torun D. Abdominopelvic tuberculosis simulating disseminated ovarian carcinoma with elevated CA-125 level: report of two cases. Abdom Imaging 2002;27:465-70.
12. Rodríguez E, Pombo F. Peritoneal tuberculosis versus peritoneal carcinomatosis: distinction based on CT findings. J Comput Assist Tomogr 1996;20:269-72.
13. Kim SH, Kim SH, Yang DM, Kim KA. Unusual causes of tubo-ovarian abscess: CT and MR imaging findings. Radiographics 2004;24:1575-89.
14. Munne KR, Tandon D, Chauhan SL, Patil AD. Female genital tuberculosis in light of newer laboratory tests: A narrative review. Indian J Tuberc 2020;67:112-20.
15. Zhang L, Weng TP, Wang HY, Sun F, Liu YY, Lin K, et al. Patient pathway analysis of tuberculosis diagnostic delay: a multicentre retrospective cohort study in China. Clin Microbiol Infect 2021;27:1000-6.
16. Tzelios C, Neuhausser WM, Ryley D, Vo N, Hurtado RM, Nathavitharana RR. Female Genital Tuberculosis. Open Forum Infect Dis 2022;9:ofac543.
17. Shah HU, Sannananja B, Baheti AD, Udare AS, Badhe PV. Hysterosalpingography and ultrasonography findings of female genital tuberculosis. Diagn Interv Radiol 2015;21:10-5.
18. Mondal SK. Histopathologic analysis of female genital tuberculosis: a fifteen-year retrospective study of 110 cases in eastern India. Turk Patoloji Derg 2013;29:41-5.
19. Epstein BM, Mann JH. CT of abdominal tuberculosis. AJR Am J Roentgenol 1982;139:861-6.
20. Pereira JM, Madureira AJ, Vieira A, Ramos I. Abdominal tuberculosis: imaging features. Eur J Radiol 2005;55:173-80.
21. Ludovisi M, De Blasis I, Virgilio B, Fischerova D, Franchi D, Pascual MA, Savelli L, Epstein E, Van Holsbeke C, Guerriero S, Czekierdowski A, Zannoni G, Scambia G, Jurkovic D, Rossi A, Timmerman D, Valentin L, Testa AC. Imaging in gynecological disease (9): clinical and ultrasound characteristics of tubal cancer. Ultrasound Obstet Gynecol 2014;43:328-35.
22. Ludovisi M, Bruno M, Capanna G, Di Florio C, Calvisi G, Guido M. Sonographic features of pelvic tuberculosis mimicking ovarian-tubal-peritoneal carcinoma. Ultrasound Obstet Gynecol 2023;61:536-8.
23. Timmerman D, Schwärzler P, Collins WP, Claerhout F, Coenen M, Amant F, Vergote I, Bourne TH.

Subjective assessment of adnexal masses with the use of ultrasonography: an analysis of interobserver variability and experience. Ultrasound Obstet Gynecol 1999;13:11-6.
24. Testa AC, Ludovisi M, Mascilini F, Di Legge A, Malaggese M, Fagotti A, Fanfani F, Salerno MG, Ercoli A, Scambia G, Ferrandina G. Ultrasound evaluation of intra-abdominal sites of disease to predict likelihood of suboptimal cytoreduction in advanced ovarian cancer: a prospective study. Ultrasound Obstet Gynecol 2012;39:99-105.
25. Moruzzi MC, Bolomini G, Esposito R, Mascilini F, Ciccarone F, Quagliozzi L, Giudice MT, Beneduce G, Ficarelli S, Moroni R, Scambia G, Fagotti A, Testa AC, Moro F. Diagnostic performance of ultrasound in assessing the extension of disease in advanced ovarian cancer. Am J Obstet Gynecol 2022;227:601.e1-601.e20.
26. Tjahyadi D, Ropii B, Tjandraprawira KD, Parwati I, Djuwantono T, Permadi W, Li T. Female Genital Tuberculosis: Clinical Presentation, Current Diagnosis, and Treatment. Infect Dis Obstet Gynecol 2022;2022:3548190.
27. Zhao T, Hu W. CA125 and HE4: Measurement Tools for Ovarian Cancer. Gynecol Obstet Invest 2016;81:430-5.

Cite this article as: Liang ZY, Zou K, Lin TL, Dong JK, Huang MQ, Zhou SM, Cai PQ, Zhang L, Li LJ. Crucial computed tomography and magnetic resonance imaging findings of fallopian tubal tuberculosis for diagnosis: a retrospective study of 26 cases. Quant Imaging Med Surg 2024;14(2):1577-1590. doi: 10.21037/qims-23-775

